

Effects of Disturbance Augmented Control Design
for Wind Turbines

TECHNICAL REPORT

Ahmet Arda Ozdemir

IN PARTIAL FULFILLMENT OF THE REQUIREMENTS
FOR THE DEGREE OF
MASTER OF SCIENCE

Gary J. Balas, Co-Adviser
Peter J. Seiler, Co-Adviser

November 2010

Abstract

The use of disturbance models in wind turbine individual pitch control design to attenuate effects of persistent disturbances is investigated. Previous work has used individual pitch control and disturbance models to design controllers that reduce the blade loads at the frequencies associated with the rotor speed. This paper takes a similar approach of using a disturbance model within the H_∞ design framework to account for periodic loading effects. The controller is compared with a baseline design that does not include the periodic disturbance model. In constant wind speeds, the disturbance model design is significantly better than the baseline design at canceling blade loads at the rotor frequencies. However, these load reduction improvements are eliminated even in low turbulent wind conditions well below limitations defined in the commonly used wind turbine design standards. The two controllers perform similarly in turbulent conditions because the turbulent wind contains energy across a broad frequency spectrum. Therefore inclusion of periodic disturbance models in the control design may not lead to the expected load reduction in fielded wind turbines.

Contents

List of Tables	iii
List of Figures	iv
Chapter 1 Introduction	1
Chapter 2 Wind Turbine Model	4
2.1 Nonlinear Wind Turbine Model	4
2.2 Linear Wind Turbine Model	6
Chapter 3 Control Problem Formulation	11
Chapter 4 Results	20
4.1 Linear Analysis	20
4.2 Nonlinear Wind Turbine Simulations	22
Chapter 5 Conclusions	32
Bibliography	34

List of Tables

2.1	Trim Conditions	7
3.1	Transformation of System Dynamics through MBC	16
4.1	Frequencies of System Modes of Interest	20
4.2	Controller Performance Comparison for Nonlinear Simulations	26

List of Figures

2.1	FAST Nonlinear System Block Diagram	6
2.2	Comparison of LTI, LTV and Nonlinear System for small perturbations	9
2.3	MBC application and Approximate LTI Turbine Model	10
2.4	Controller Implementation of on nonlinear system	10
3.1	System Interconnection for H_∞ Rotor Speed Controller Design	12
3.2	Frequency spectrum of 5% turbulent wind and W_{dist} input weight . .	13
3.3	Bode Plots from Wind Disturbance to Rotor Speed Deviation	14
3.4	System Interconnection for H_∞ Individual Pitch Controller Design . .	15
3.5	Frequency spectrum of output trim trajectories and disturbance models	19
4.1	Bode Plots from Wind Disturbance to M_{tilt}^{nr}	21
4.2	Bode Plots from Wind Disturbance to M_{yaw}^{nr}	22
4.3	Open and Closed Loop Bode Plots for disturbance on M_{tilt}^{nr} to M_{tilt}^{nr} .	23
4.4	Open and Closed Loop Bode Plots for disturbance on M_{yaw}^{nr} to M_{yaw}^{nr} .	24
4.5	Hub-height wind disturbances used in simulations	25
4.6	PSD of Blade 1 Root Bending Moment under steady wind conditions	27
4.7	PSD of Blade 1 Root Bending Moment under 1% turbulent wind . . .	28
4.8	PSD of Blade 1 Root Bending Moment under 5% turbulent wind . . .	29

4.9	The PSD of M_{avg} Channel	30
4.10	The PSD of M_{tilt} Channel	31

Chapter 1

Introduction¹

Demand for renewable energy is increasing rapidly with many governments setting aggressive goals towards greener energy alternatives. Wind energy plays an important role in this development as a promising renewable energy source and its success depends on the competitiveness of its cost per unit energy. The economics of wind power generation has driven the wind power industry to turbines of enormous size. Several issues arise due to the large dimensions including increased flexibility of the tower and blades and increased coupling between the turbine modes. Advanced control algorithms can be used to address vibration and loading issues, especially at above-rated wind speeds, and thus result in better fatigue reduction and lower maintenance costs.

A wind turbine operating in above-rated wind speeds (region 3) has the control objective of maintaining its rated power while minimizing structural loads on its blades, tower and the gearbox system. Turbulent wind conditions as well as persistent disturbances such as vertical wind shear, gravity and tower shadow are typical disturbances acting on the turbine. Conventionally, single-input single-output (SISO) classical control methods involving independent control loops are used for wind turbine control. A PID controller commanding collective blade pitch can be used to track desired constant rotor speed, while the generator torque is set accordingly to obtain rated power of the turbine. The generator torque command can be modified to add damping to the drive train torsion vibrations while collective pitch command can be modified to

¹This technical report has been submitted to the Journal of Mechatronics for publication on September, 2010:

Ozdemir, A. A., Seiler, P., and Balas, G. J., Effects of Disturbance Augmented Control Design for Wind Turbines, Submitted to the Journal of Mechatronics.

damp out tower fore-aft vibrations [1]. In addition to the SISO approaches, various multi-input multi-output (MIMO) control techniques such as Linear Quadratic Gaussian [2] and H_∞ [3] using individual pitch control (IPC) also have been investigated in the literature.

In addition to these methods, there are also MIMO controllers in the literature that are designed to eliminate the effects of persistent disturbances for load reduction. These controllers either use an observer to estimate the disturbances on the turbine in real time or include models of disturbances at the design stage of the controller. One common example of the estimator based approach is Disturbance Accommodating Control (DAC) [4–6]. DAC is an extension of LQR control that is based on estimating the persistent disturbances acting on the turbine. An example of the controllers that account for the effects persistent disturbances at design stage can be found in [7]. With this method, disturbance models are augmented to the plant output to model the effects of the disturbances on system outputs. Instead of estimating the disturbances directly, the undesired effect of disturbances on system outputs are considered and controllers are designed to attenuate these effects.

All these linear control approaches require a linear representation of the nonlinear wind turbine system. The turbine is subjected to time-varying loads even in constant wind conditions because persistent disturbances such as tower shadow, gravity, shaft tilt e.g. and aerodynamic forces depend on the rotor position and structural flexibility. As a result, the wind turbine trim values are time-varying and periodic even in constant wind conditions. The amplitudes of these time-varying oscillations are significant for larger, more flexible turbines. The periodic behavior depends on the rotor position. Linearizations computed at each rotor position results in a periodic, linear time-varying (LTV) system with period equal to the rotor rotation period.

It is often desirable to transform the LTV control problem into an equivalent LTI problem to make use of well established linear time invariant (LTI) control techniques. There are various methods available in literature to obtain a LTI model from a LTV system. The simplest approach is to evaluate the periodic LTV system at a single constant rotor position. This approach ignores the periodic modal characteristics of the turbine and may not represent the nonlinear model well enough depending on the control problem. Averaging the state matrices over a single rotor period is another straightforward approach but there are no methods to determine the quality

of model approximation [8]. Floquet theory [9] can be used to obtain a time-varying coordinate transformation that transforms a periodic LTV system into an LTI system while retaining all of the periodic modal characteristics. A drawback is that any physical intuition about the system states is lost during Floquet transformation. In this case, the eigenvectors of the resulting LTI system can be approximately related to the modes of the the physical system. Another modeling approach is to use the multi-blade coordinate (MBC) transformation [9,10] to express the states, inputs and outputs of the turbine in a non-rotating coordinate frame. In general the MBC transformation does not directly result in an LTI system. However, the MBC approach usually yields a model that is weakly periodic and averaging of system matrices can result in a LTI model of sufficient accuracy [11]. The MBC transformation is also known as the Coleman transformation or Fourier coordinate transformation in literature. Note that a reduced form of the MBC transform, called the $d - q$ transform, has also been applied to wind turbine control problems [2].

In this paper, the effects of disturbance model augmentation are investigated for a standard Region 3 controller design. A periodic LTV system model of the nonlinear wind turbine dynamics is obtained by linearization of the wind turbine model as a function of the rotor angle. The periodic LTV system is approximated by an LTI system using the MBC transformation and averaging the resulting state matrices over one rotor rotation period. Oscillations in the trim operating values are modeled as disturbances of known frequencies and magnitudes acting on the output of the linear system. A H_∞ optimal controller designed on the disturbance augmented plant is compared with a baseline design that does not include the periodic disturbance model.

The paper has the following structure: Section 2 describes the nonlinear model used in this paper and explains the derivation of the LTI model. Section 3 explains the control problem formulation and design in detail. The linear analysis and nonlinear simulation results are presented in Section 4. Conclusions are presented in Section 5.

Chapter 2

Wind Turbine Model

2.1 Nonlinear Wind Turbine Model

Nonlinear simulations presented in this work are performed using FAST [12], which stands for Fatigue, Aerodynamics, Structures and Turbulence modeling. FAST is a publicly available nonlinear aeroelastic turbine simulation code developed by National Renewable Energy Laboratory. FAST uses the assumed modes method for the flexible structural dynamics of the system. Blade element momentum theory is used to calculate the aerodynamic loads using AeroDYN [13]. The wind turbine considered in this paper is the WindPACT 1.5MW horizontal axis, 3-bladed upwind turbine whose parameters are distributed with the FAST package.

FAST can model onshore wind turbines with a total of 16 degrees of freedom (DOF). This full order model includes first and second tower fore-aft and side-to-side bending modes, first and second flapwise bending modes of blades, first edgewise bending modes of blades, drivetrain torsion, generator position and nacelle yaw angle. Only a subset of these available DOF are chosen for the control design to reduce the complexity of the design. First, the yaw dynamics of the system are ignored since typically yaw motion and yaw actuators have time constants considerably larger than pitch actuators and generator torque control. Generator torque is not included as a control input and is held constant in this individual pitch control study. High frequency dynamics of the system that lie beyond the bandwidth of pitch actuators are also eliminated since the pitch actuators do not have enough control authority on these dynamics. These neglected dynamics include first edgewise and second flapwise bend-

ing modes of the blades, second tower fore-aft and side-to-side bending modes and drivetrain torsion. The final step is to eliminate the tower first side-to-side mode for the scope of this work. Even though IPC algorithms can affect this mode, side-to-side motion has limited effect on blade fatigue and it is eliminated for model reduction. During the control design no performance demands are imposed on the modes deleted from the system. The resulting simplified five degree-of-freedom system includes rotor position, first tower fore-aft bending mode and first flapwise bending mode for each blade. Note that the collective pitch action has a significant effect on tower fore-aft motion and in order to avoid destabilizing this lightly damped mode it is important to include it in control design [1]. This reduced order linear model is used for control design. Simulations are performed on high order nonlinear turbine model.

The five DOF nonlinear wind turbine modeled in FAST is represented by Equations (2.1) and (2.2). A block diagram of the wind turbine model is shown in Figure 2.1.

$$\ddot{q} = f(\dot{q}, q, u, F, t) \quad (2.1)$$

$$y = g(\dot{q}, q, u, F, t) \quad (2.2)$$

where $q \in R^5$ and $\dot{q} \in R^5$ are the turbine states, $u \in R^4$ is the control input, $F \in R^1$ is the wind disturbance and $y \in R^4$ is the measurement vector. The variables are defined as:

$$q = \begin{bmatrix} q_1 \\ \psi_r \\ q_3 \\ q_4 \\ q_5 \end{bmatrix} = \begin{bmatrix} \text{Tower 1}^{st} \text{ Fore-Aft Bending Mode Tip Disp. (m)} \\ \text{Rotor position from Blade 1 Upwards Position (rad)} \\ \text{Blade 1 1}^{st} \text{ Flapwise Bending Mode Tip Disp. (m)} \\ \text{Blade 2 1}^{st} \text{ Flapwise Bending Mode Tip Disp. (m)} \\ \text{Blade 3 1}^{st} \text{ Flapwise Bending Mode Tip Disp. (m)} \end{bmatrix} \quad (2.3)$$

$$u = \begin{bmatrix} \theta_1 \\ \theta_2 \\ \theta_3 \end{bmatrix} = \begin{bmatrix} \text{Blade 1 Pitch Angle (rad)} \\ \text{Blade 2 Pitch Angle (rad)} \\ \text{Blade 3 Pitch Angle (rad)} \end{bmatrix} \quad (2.4)$$

$$F = [V_w] = [\text{Horizontal Hub-Height Wind Speed (m/s)}] \quad (2.5)$$

$$y = \begin{bmatrix} \Omega \\ M_1 \\ M_2 \\ M_3 \end{bmatrix} = \begin{bmatrix} \text{Rotor Speed (rpm)} \\ \text{Blade 1 Bending Moment at Blade Root (kN m)} \\ \text{Blade 2 Bending Moment at Blade Root (kN m)} \\ \text{Blade 3 Bending Moment at Blade Root (kN m)} \end{bmatrix} \quad (2.6)$$

The generator torque input is held constant in this study hence it is not listed in the vector u in Eq. 2.4. The system outputs, vector y in Eq. 2.6, are selected to include a realistic sensor configuration for the study. Rotor speed measurement is commonly available on turbines and load sensors are becoming more popular due to their increasing reliability and low costs. In addition, implementation of controllers obtained through the MBC transformation requires knowledge of the rotor position even though it is not included in y measurement vector described. Rotor position measurement is also readily available in many turbines.

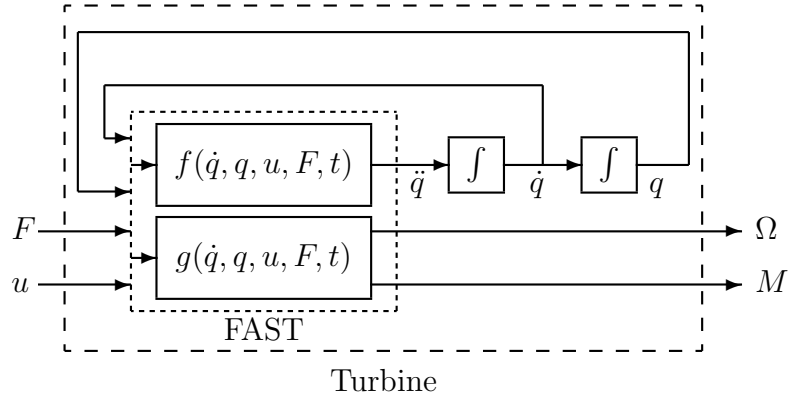


Figure 2.1: FAST Nonlinear System Block Diagram

2.2 Linear Wind Turbine Model

FAST has the capability of producing linear turbine models through numerical perturbation of system equations (2.1) and (2.2). The nonlinear system is first simulated under steady wind conditions until the turbine reaches a trim operating trajectory. The system is linearized around this trim trajectory. The trim operating condition is a periodic trajectory $\bar{q}(t)$ that satisfies Equation (2.7).

$$\begin{aligned} \ddot{\bar{q}} &= f(\dot{\bar{q}}, \bar{q}, \bar{u}, \bar{F}, t) \\ \bar{y} &= g(\dot{\bar{q}}, \bar{q}, \bar{u}, \bar{F}, t) \end{aligned} \quad (2.7)$$

$\bar{q}(t)$ is periodic in the rotor rotation period T , i.e. $\bar{q}(t + T) = \bar{q}(t)$. The wind input \bar{F} and blade pitch angles \bar{u} are held fixed at the trim values specified in Table 2.1. If the oscillations in \bar{q} have small amplitude, the average state over one period can be assumed to be a constant trim condition without introducing large errors [14]. The effect of the periodic trajectory is not neglected in this paper. Rather, it is included as a periodic disturbance on the turbine. A linear time-varying model is obtained by linearizing the nonlinear system (Equations (2.1) and (2.2)) around $\bar{q}(t)$. The resulting equations have the form of Equation (2.8).

$$\begin{aligned}\dot{x} &= A(\bar{\psi}_r(t))x + B(\bar{\psi}_r(t))\Delta u + B_d(\bar{\psi}_r(t))\Delta F \\ \Delta y &= C(\bar{\psi}_r(t))x + D(\bar{\psi}_r(t))\Delta u + D_d(\bar{\psi}_r(t))\Delta F\end{aligned}\tag{2.8}$$

where

$$\begin{aligned}x &= \begin{bmatrix} \Delta q \\ \Delta \dot{q} \end{bmatrix} = \begin{bmatrix} q - \bar{q} \\ \dot{q} - \dot{\bar{q}} \end{bmatrix} \\ \Delta u &= u - \bar{u} \\ \Delta F &= F - \bar{F} \\ \Delta y &= y - \bar{y} = \begin{bmatrix} \Delta \Omega \\ \Delta M_1 \\ \Delta M_2 \\ \Delta M_3 \end{bmatrix}\end{aligned}\tag{2.9}$$

Since the trim trajectories are periodic, $\bar{\psi}_r(t) = \bar{\psi}_r(t + T)$, the system equations given by Equation (2.8) are also periodic. The operating conditions used for the linearization are listed in Table 2.1.

Table 2.1: Trim Conditions

Description	Value
Mean wind speed, \bar{F}	18.0 m/s
Vertical shear factor	0.2
Rotor speed, $\bar{\Omega}$	2.15 rad/s
Collective blade pitch, \bar{u}	0.3352 rad
Generator torque (High Speed Side)	8377.0 Nm

The linear and nonlinear wind turbine equations of motion presented are derived

using a variety of coordinate frames. While quantities associated with the tower and rotor are expressed in an earth fixed coordinate frame, quantities that belong to individual blades are defined in a frame that rotates with the rotor. For instance, blade flapwise bending mode tip displacements are defined with respect to a rotating coordinate frame attached to the blade. The MBC transformation takes the system states, inputs and outputs defined in a mixed coordinate system (both rotating and non-rotating) and expresses them in a purely non-rotating coordinate frame.

The triplets of states, inputs, and outputs of the linear system that are expressed in a rotating frame are transformed as:

$$\begin{bmatrix} q_3^{nr} \\ q_4^{nr} \\ q_5^{nr} \end{bmatrix} = \mathbf{T}^{-1}(\bar{\psi}_r(t)) \begin{bmatrix} q_3 \\ q_4 \\ q_5 \end{bmatrix}, \quad \begin{bmatrix} \theta_1^{nr} \\ \theta_2^{nr} \\ \theta_3^{nr} \end{bmatrix} = \mathbf{T}^{-1}(\bar{\psi}_r(t)) \begin{bmatrix} \theta_1 \\ \theta_2 \\ \theta_3 \end{bmatrix}, \quad \begin{bmatrix} M_{avg}^{nr} \\ M_{tilt}^{nr} \\ M_{yaw}^{nr} \end{bmatrix} = \mathbf{T}^{-1}(\bar{\psi}_r(t)) \begin{bmatrix} M_1 \\ M_2 \\ M_3 \end{bmatrix} \quad (2.10)$$

where

$$\mathbf{T}^{-1}(\bar{\psi}_r(t)) = \frac{1}{3} \begin{bmatrix} 1 & 1 & 1 \\ 2 \sin(\bar{\psi}_r(t)) & 2 \sin(\bar{\psi}_r(t) + 2\pi/3) & 2 \sin(\bar{\psi}_r(t) + 4\pi/3) \\ 2 \cos(\bar{\psi}_r(t)) & 2 \cos(\bar{\psi}_r(t) + 2\pi/3) & 2 \cos(\bar{\psi}_r(t) + 4\pi/3) \end{bmatrix} \quad (2.11)$$

$$\mathbf{T}(\bar{\psi}_r(t)) = \begin{bmatrix} 1 & \sin(\bar{\psi}_r(t)) & \cos(\bar{\psi}_r(t)) \\ 1 & \sin(\bar{\psi}_r(t) + 2\pi/3) & \cos(\bar{\psi}_r(t) + 2\pi/3) \\ 1 & \sin(\bar{\psi}_r(t) + 4\pi/3) & \cos(\bar{\psi}_r(t) + 4\pi/3) \end{bmatrix} \quad (2.12)$$

The superscript nr denotes quantities expressed in non-rotating frame. After the transformation, these quantities have meanings in terms of rotor motion instead of individual blades. M_{avg}^{nr} represents average value of blade root bending moments and causes the rotor to bend as a cone. M_{tilt}^{nr} represents the moment from blades resulting in rotor tilt, and similarly M_{yaw}^{nr} is the moment in the yaw direction of rotor [15]. q_1^{nr} , q_2^{nr} , q_3^{nr} are defined as rotor coning, rotor tip-path-plane fore-aft tilt and rotor tip-path-plane side-side tilt, respectively [16]. θ_1^{nr} is the collective pitch command, while θ_2^{nr} and θ_3^{nr} are cyclic individual blade pitch commands.

The resulting state space matrices derived with the MBC transformation usually have significantly less variation due to rotor position. Averaging these small amplitude variations in the periodic matrices generally yields acceptable results even with extreme wind conditions where the effects of periodicity are highest [11]. Controllers

can be designed based on the resulting LTI approximation. A comparison of the LTI model used for control design and the periodic LTV and nonlinear system models are presented in Figure 2.2. Figure 2.2 shows the response of these models to a small perturbation in collective pitch input in rotating frame. The inputs and outputs of the LTI system is transformed through MBC and inverse MBC to obtain the system response in rotating frame. Note that there is excellent correlation between the response except for the amplitude of the oscillations.

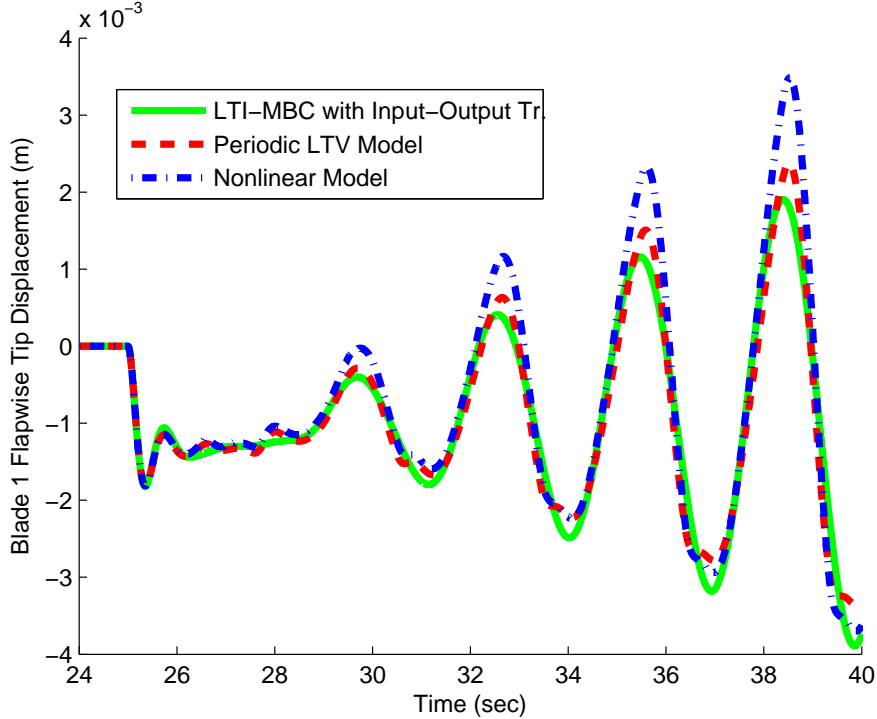


Figure 2.2: Comparison of LTI, LTV and Nonlinear System for small perturbations

Since the LTI approximation is obtained with fictitious input-output MBC transformations, these transformations must be implemented as a part of the controller on turbine. The LTI approximation of the periodic LTV system is shown in Figure 2.3 and the resulting periodic gain controller interconnection is shown in Figure 2.4. The inputs of the controller in the nonlinear simulations are $\Delta\Omega$, ΔM_{avg}^{nr} , M_{tilt}^{nr} , M_{yaw}^{nr} since these are the signals to be attenuated.

The MBC transformation is a function of the trim trajectory of rotor position. When implemented, the rotor position of the actual turbine will diverge from its trim trajectory due to varying wind conditions. Hence it is desired to use the actual rotor

position, i.e. $\mathbf{T}(\psi_r(t))$ rather than $\bar{\mathbf{T}}(\psi_r(t))$, for the MBC transformation as discussed in the previous section. Further details of MBC can be found in [16], along with its application to numerical linearization data obtained through simulation codes.

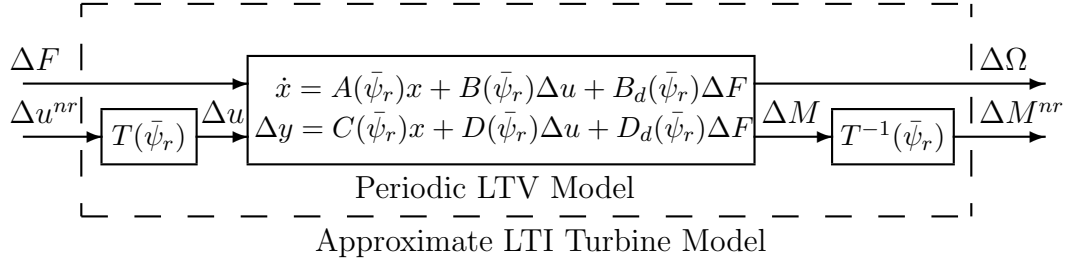


Figure 2.3: MBC application and Approximate LTI Turbine Model

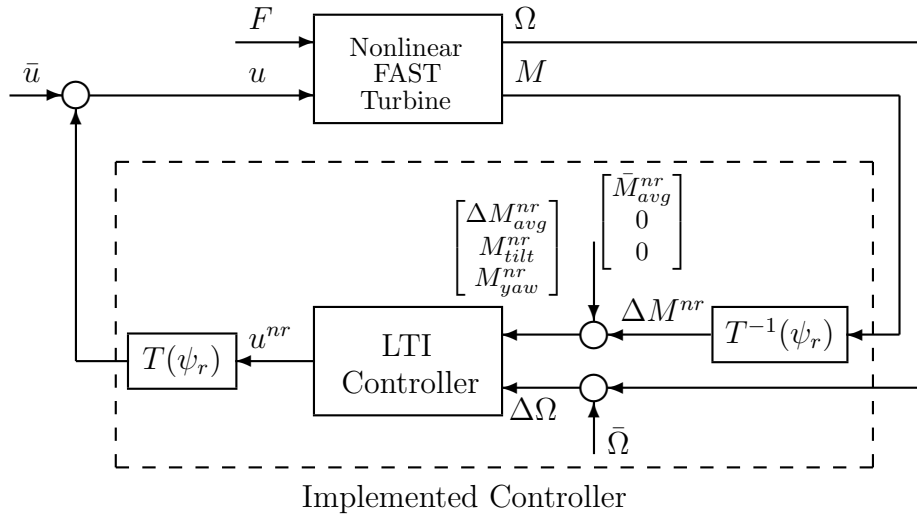


Figure 2.4: Controller Implementation of on nonlinear system

Chapter 3

Control Problem Formulation

Wind turbine control in Region 3 involves minimizing loads on the turbine structure and rotor speed deviations from the rated speed. A wind turbine is subject to turbulent wind disturbances, as well as persistent disturbances like gravity, tower shadow and wind shear. These persistent disturbances coupled with the rotor rotation result in a significant contribution to the $1p$ loads on the rotating structures and $3p$ loads on the non-rotating structures where np is defined as the n -th multiple of the rotor rotation frequency. Due to coupling of persistent disturbances and rotor rotation, a turbine operating under constant wind conditions still has oscillations in its trim trajectory (see Section 2.2). It is often desired to account for these persistent disturbances in addition to the standard load reduction problem into control problem formulation to further reduce loads on the turbine. Disturbance models are often used in literature for individual pitch control in order to attenuate effects of the disturbances on the turbine [7].

A two layered design procedure is used for regulating rotor speed and blade loads in this paper. The first layer consists of a rotor speed controller that uses rotor speed measurement to generate collective pitch commands. An individual pitch controller is designed for blade load reduction with the rotor speed controller implemented. The IPC takes M_{avg}^{nr} , M_{tilt}^{nr} and M_{yaw}^{nr} measurements to generate cyclic pitch commands. To investigate the potential improvements that can be achieved through disturbance model augmentation, two IPC are designed using H_∞ ([17], [18]) control design techniques. The first IPC design uses the disturbance model and the other baseline design does not. Both IPC designs share the same rotor speed controller. The reason

for selecting a two layered design is to get similar rotor speed tracking and tower fatigue characteristics for a fair comparison of blade load reduction characteristics of the IPC algorithms. The decoupling of the control problem is not expected to impact the problem studied since the load reduction improvement by disturbance model augmentation is expected solely through cyclic pitch commands. On the other hand, it should be noted that the two layer approach does not take into account all the couplings in the system as well as the tradeoff between rotor speed tracking and load reduction problems. A single controller that accounts for all the couplings in the system can result better overall performance.

For the H_∞ control problem, performance requirements for the turbine and controller are expressed in the frequency domain by selecting appropriate weights on system signals. The H_∞ control design approach used in this paper is built on the results of [3]. The system interconnection used for rotor speed control is shown in Figure 3.1.

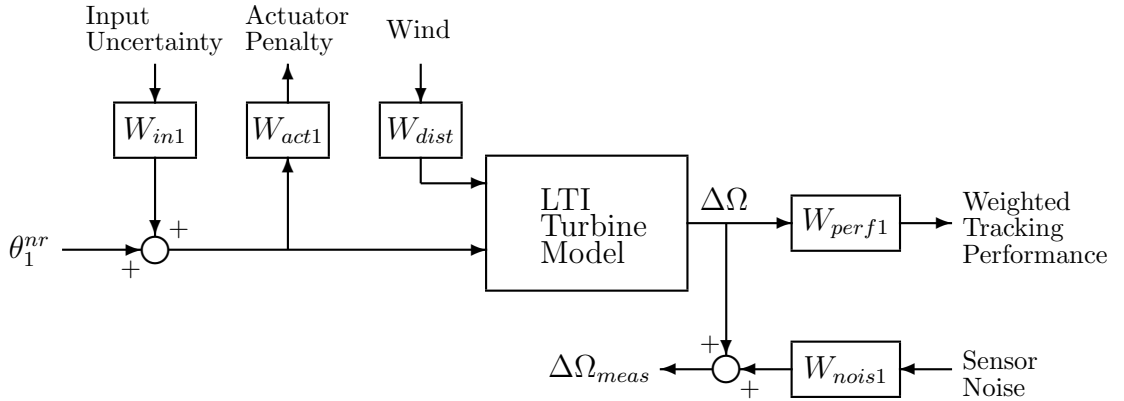


Figure 3.1: System Interconnection for H_∞ Rotor Speed Controller Design

W_{dist} models the characteristics of the expected turbulent wind disturbances. The wind conditions are assumed to consist of 5% turbulence intensity on top of the steady wind conditions specified in Table 2.1. According to the The International Electrotechnical Commission (IEC) IEC-61400-1 standards [19, 20], 5% turbulence is defined as low turbulent wind conditions. Typically, class C wind turbines designed for low turbulence conditions must be able to operate in 13% wind turbulence whereas class B and A wind turbines must withstand higher turbulence levels. Wind input data with 5% turbulence over steady wind conditions was generated using TurbSim [21], a stochastic, turbulent wind simulator. Since the input of the linear system is the deviation from steady wind conditions, the mean wind speed is subtracted from

the raw data. The frequency spectrum is obtained using a Discrete Fourier Transform and its spectrum is overbounded with a transfer function to obtain W_{dist} . A Bode plot of W_{dist} and the frequency spectrum of the wind data are shown in Figure 3.2. The resulting W_{dist} is given in Eq. 3.1.

$$W_{dist}(s) = 0.25 \frac{1/60s + 1}{1/4s + 1} \quad (3.1)$$

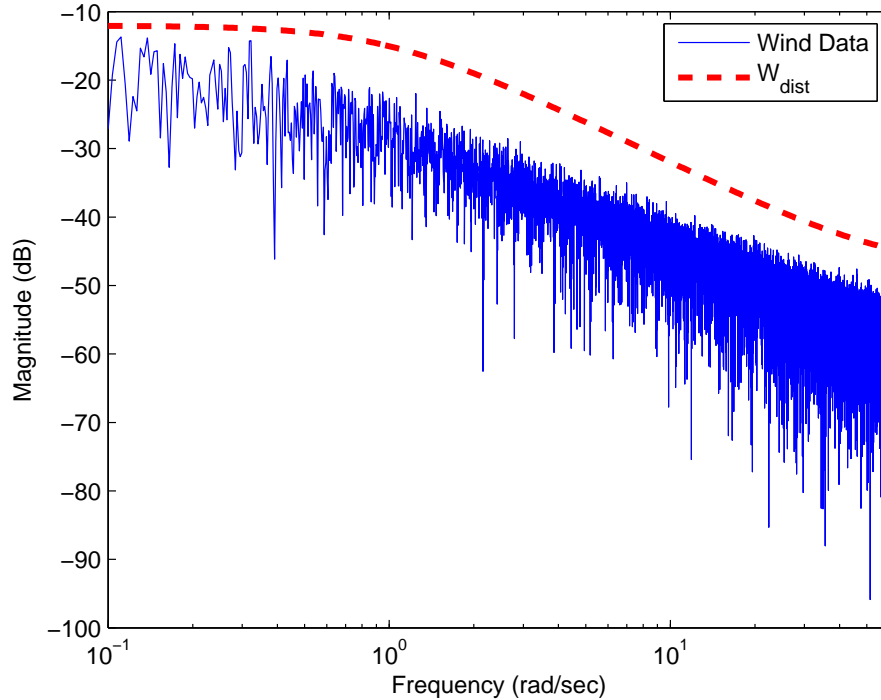


Figure 3.2: Frequency spectrum of 5% turbulent wind and W_{dist} input weight

The rotor speed tracking problem involves minimizing the deviations from the rated rotor speed. This can be achieved by attenuating the gain from wind disturbances to rotor speed deviation output $\Delta\Omega$. The open loop Bode plot from wind disturbance to $\Delta\Omega$ is given in Figure 3.3. Figure 3.3 also contains closed loop results that will be discussed later. It can be seen that the poorest disturbance attenuation occurs at low frequencies and there is a valley at tower natural frequency. It is desired to improve the attenuation in this channel especially at low frequencies where the wind disturbance input has the highest gain. Since the system is rolling off quickly at frequencies beyond actuator bandwidth, a constant inverse weight $W_{perf1} = 1$ is chosen for W_{perf1} such that worse case deviation is 1 rpm. The main limitations

on this objective are the coupling between tower fore-aft motion and the actuator bandwidth. Note that the controller should have a notch characteristic at the tower bending mode frequency to avoid exciting tower motion.

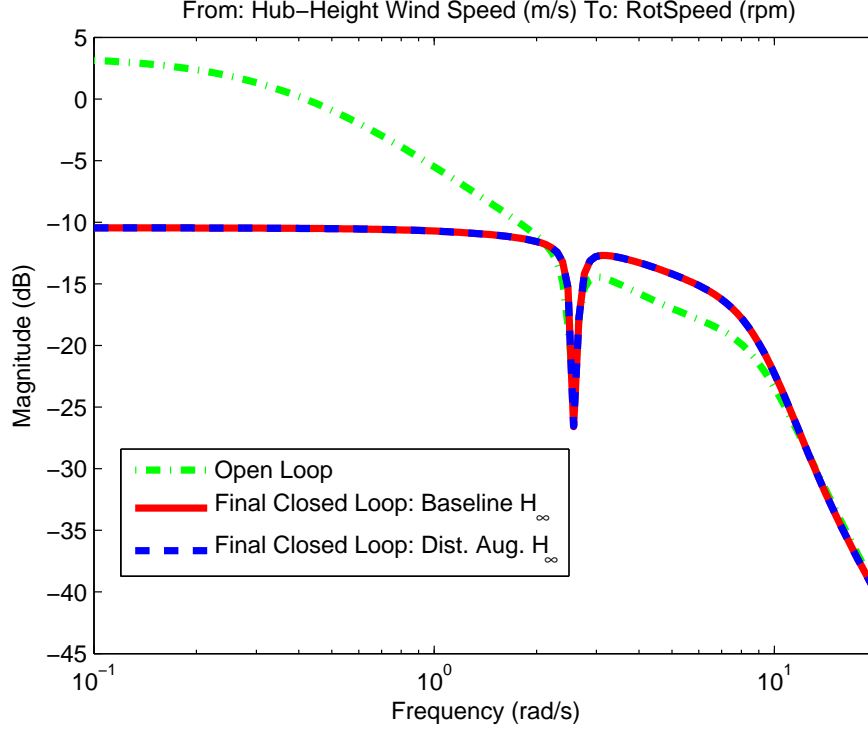


Figure 3.3: Bode Plots from Wind Disturbance to Rotor Speed Deviation

W_{act1} is the actuator penalty on the collective pitch command. The actuators on the turbine are considered to have pitch rate limitations of 0.1745 rad/s and bandwidth limitations of 10 rad/s. The actuator commands in rotating frame are transformed to nonrotating frame through $\theta^{nr} = \mathbf{T}^{-1}(\psi_r(t))\theta$ in time domain. In the frequency domain this corresponds to convolution. Hence it is non-trivial to precisely relate weights in rotating coordinates to nonrotating coordinates. Understanding the effect of an MBC transformation on the actuator signals is an open research topic which is not addressed in this research. For the scope of this study, a simpler but less precise approach was taken. A first order weight is chosen with the zero at $s = -10$ and the pole at $s = -80$ to penalize high frequency controller action. The gain of the weight is adjusted after a few iterations observing actuator signals in the nonlinear simulations. It has been validated that the actuator demands do not exceed physical actuator limits. The weight $W_{act1}(s)$ used in design is given in Eq. 3.2.

$$W_{act1}(s) = \frac{8}{\pi} \frac{1/10s + 1}{1/80s + 1} \quad (3.2)$$

An input uncertainty is added to the collective pitch command through the weight $W_{in1} = 0.01$ to model the difference between controller commands and actuator outputs. This value of W_{in1} typically corresponds to about 1% of the collective pitch commands expected by the controller. W_{nois1} was chosen to be 0.021. This approximately models noise with amplitude equal to 1% of rated rotor speed.

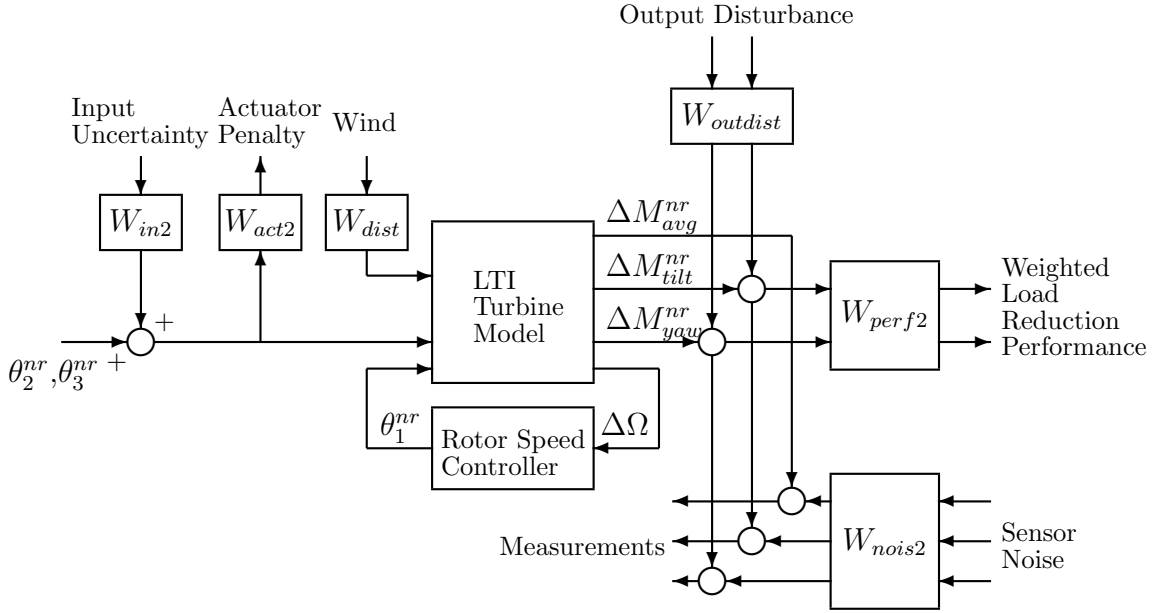


Figure 3.4: System Interconnection for H_∞ Individual Pitch Controller Design

The IPC design interconnection is presented in Figure 3.4. The wind turbine structural loads occur mostly at integer multiples of the rotor frequency due to rotation dynamics. Blade fatigue is dominated by the $1p$ dynamics of the turbine though the effects of the $2p$, $3p$ and $4p$ dynamics can be important to some extent where p is the rotor rotation frequency. These np rotation dynamics can be observed in $[M_1; M_2; M_3]$ blade bending loads as three sinusoidals with $\frac{2n\pi}{3}rad$ phase shift in between. In order to account for these loads observed in physical coordinates, the corresponding signals in nonrotating frame must be obtained through MBC transformation presented in

Equation 3.3.

$$\begin{bmatrix} M_{avg}^{nr} \\ M_{tilt}^{nr} \\ M_{yaw}^{nr} \end{bmatrix} = \mathbf{T}^{-1}(\bar{\psi}_r(t)) \begin{bmatrix} \sin(npt) \\ \sin(n(pt + \frac{2\pi}{3})) \\ \sin(n(pt + \frac{4\pi}{3})) \end{bmatrix} \quad (3.3)$$

Transformation of some of the important rotation dynamics are summarized in Table 3.1. The superscript nr is used when frequencies and quantities expressed in nonrotating frame are referred. For instance, in order to reduce loads caused by $1p$ dynamics of the system, $0p^{nr}$ (DC component) of M_{tilt}^{nr} and M_{yaw}^{nr} must be penalized. For reduction of loads caused by $2p$ and $4p$ dynamics of rotation, the $3p^{nr}$ of M_{tilt}^{nr} and M_{yaw}^{nr} must be penalized. The traditional IPC problem usually ignores the M_{avg}^{nr} channel since individual pitch control has limited effect on this channel. Hence it is seen that loads caused by $3p, 6p, 9p\dots$ dynamics are not accounted when M_{avg}^{nr} is neglected. It should be noted that Table 3.1 only summarizes transformation of wind turbine rotating dynamics which consist of three sinusoidals at np frequency with $\frac{2n\pi}{3}$ phase shifts; and not the transformation of any arbitrary three sinusoidals at np frequency.

Table 3.1: Transformation of System Dynamics through MBC

Rotating Frame Dynamics	Nonrotating Frame
$1p$, separated by $\frac{2\pi}{3}rad$	$0p^{nr}$ (DC) @ M_{tilt}^{nr} and M_{yaw}^{nr}
$2p$, separated by $\frac{4\pi}{3}rad$	$3p^{nr}$ @ M_{tilt}^{nr} and M_{yaw}^{nr}
$3p$, separated by $0rad$	$3p^{nr}$ @ M_{avg}^{nr}
$4p$, separated by $\frac{2\pi}{3}rad$	$3p^{nr}$ @ M_{tilt}^{nr} and M_{yaw}^{nr}
$5p$, separated by $\frac{4\pi}{3}rad$	$6p^{nr}$ @ M_{tilt}^{nr} and M_{yaw}^{nr}
$6p$, separated by $0rad$	$6p^{nr}$ @ M_{avg}^{nr}
$7p$, separated by $\frac{2\pi}{3}rad$	$6p^{nr}$ @ M_{tilt}^{nr} and M_{yaw}^{nr}

The block diagonal performance weight W_{perf2} contains two first order weights for yaw and tilt moments to reflect the performance demands of reducing loads at $0p^{nr}$ and low frequencies in nonrotating frame. This represents the demand of reducing $1p$ loads as well as other low frequency components of the blade loads caused by turbulent wind conditions in rotating frame. Velocity and acceleration limits on the actuators play a large role in this objective, and commonly compensation on modes beyond the $3p$ or $4p$ frequencies are avoided to prevent exciting blade bending modes and other high-order system dynamics. It should be noted that the choice of performance weights do not penalize the $3p^{nr}$ frequency. Hence it is expected that the controller

will not provide significant improvements for $2p$ and $4p$ loads. The weight $W_{perf2}(s)$ used in design is given in Eq. 3.4.

$$W_{perf2} = 0.032 \begin{bmatrix} \frac{1}{1/0.05s+1} & 0 \\ 0 & \frac{1}{1/0.05s+1} \end{bmatrix} \quad (3.4)$$

W_{nois2} is chosen as a block diagonal constant weight to incorporate the noise on blade bending moment sensors transformed to nonrotating frame. Its gain is chosen to be 1% of their values at trim operating condition. W_{act2} is chosen as a first order weight for the actuator penalty on cyclic pitch commands to limit the bandwidth of the compensation. The values of W_{nois2} and W_{act2} are given in Equations 3.5 and 3.6 respectively. $W_{in2} = \begin{bmatrix} 0.01 & 0 \\ 0 & 0.01 \end{bmatrix}$ is the input uncertainty on cyclic pitch commands. W_{in2} is included to model the difference between actuator outputs and controller commands.

$$W_{nois2} = \begin{bmatrix} 6 & 0 & 0 \\ 0 & 1.5 & 0 \\ 0 & 0 & 1.5 \end{bmatrix} \quad (3.5)$$

$$W_{act2}(s) = \frac{3}{\pi} \begin{bmatrix} \frac{1/10s+1}{1/80s+1} & 0 \\ 0 & \frac{1/10s+1}{1/80s+1} \end{bmatrix} \quad (3.6)$$

The output disturbances are modeled based on the trim trajectory of the system. The trim trajectory of the wind turbine is considered to be a result of persistent disturbances, which is undesirable, acting on the turbine. Trajectories of the system outputs \bar{y} are obtained during simulation and expressed in the original (rotating) coordinate frame. To incorporate this information into the controller design procedure in the non-rotating frame, the MBC transformation is applied on $\bar{y}(t)$ to obtain $\bar{y}^{nr}(t)$ in the nonrotating frame. Here only \bar{M}_{tilt}^{nr} and \bar{M}_{yaw}^{nr} are modeled as output disturbances to represent the moments in tilt and yaw direction. The variations observed in the rotor speed trajectory are negligible due to large inertia of the rotor. Similarly, \bar{M}_{avg}^{nr} has small variations with respect to rotor position and is not included. A Discrete Fourier Transform of \bar{M}_{tilt}^{nr} and \bar{M}_{yaw}^{nr} is obtained and these are overbounded with transfer functions $G_1(s) = \frac{132.1s^2 + 561.4s + 5479.0}{10s^3 + 1.388s^2 + 414.9s + 4.149}$ and

$G_2(s) = \frac{-129.8s^2 - 551.7s - 5384.0}{10s^3 + 1.388s^2 + 414.9s + 4.149}$ respectively. Then the output disturbance model is chosen as $W_{outdist}(s) = \gamma \begin{bmatrix} G_1(s) & 0 \\ 0 & G_2(s) \end{bmatrix}$ with $\gamma = 10$ to ensure that the H_∞ optimization is focused on the output disturbances.

The disturbance models used for \bar{M}_{tilt}^{nr} and \bar{M}_{yaw}^{nr} are shown in Figure 3.5. In the H_∞ framework, these disturbance models are driven by bounded L_2 signals. A scalar signal $u(t)$ is in L_2 if $\|u\|_2 < \infty$ where the 2-norm of $u(t)$ is defined as:

$$\|u\|_2 := \left(\int_0^{+\infty} u(t)^2 dt \right)^{1/2}$$

If $\exists M, T < \infty$ such that $|u(t)| < M \forall t \in [0, T]$ and $u(t) = 0$ for $t > T$, then $u(t) \in L_2$. Hence bounded L_2 signals can provide a reasonable representation for persistent disturbances encountered in any finite-time experiment.

In the literature, a similar approach to the approach presented here is given in [7], where a disturbance model driven by linear system outputs was augmented to the control problem. A similar approach to modeling of the blade load reduction problem as an output disturbance rejection has also been investigated in the helicopter control literature [22].

The interconnection presented in Figure 3.1 is used to design a rotor speed controller. The disturbance augmented H_∞ individual pitch controller was designed using the interconnection in Figure 3.4. The baseline H_∞ IPC was designed using the same interconnection but without the output disturbance model. The weighting functions used are given in the Appendix section. The resulting H_∞ norm of the closed-loop interconnection for both IPC designs were less than 1 which means performance objectives specified as defined by the weights are achieved.

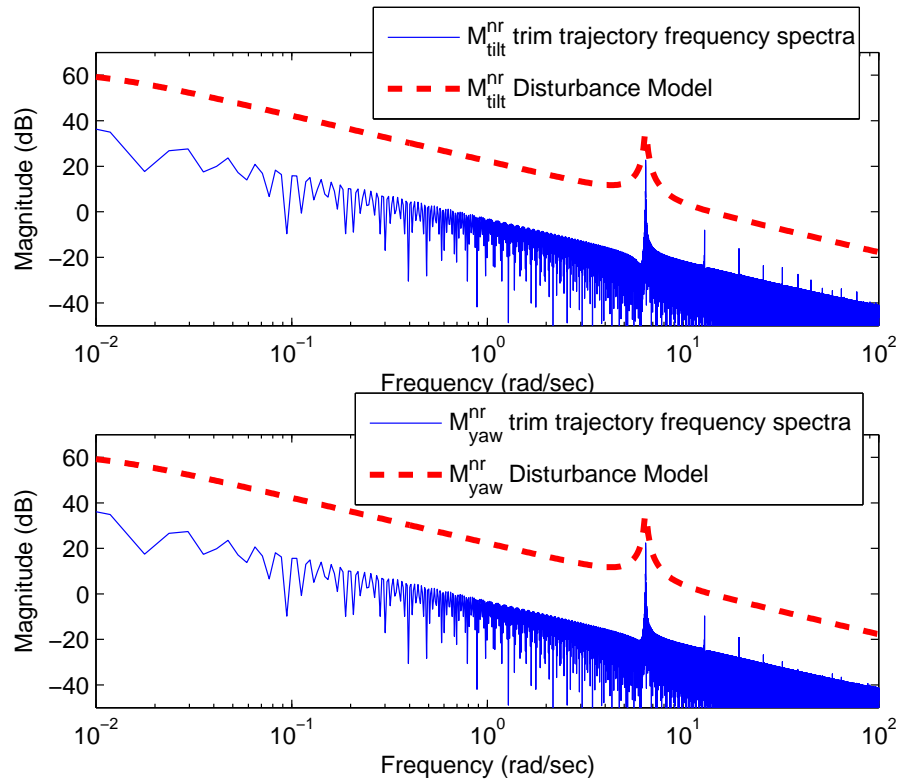


Figure 3.5: Frequency spectrum of output trim trajectories and disturbance models

Chapter 4

Results

4.1 Linear Analysis

This section compares the two closed-loop systems using linear analysis. Table 4.1 lists the frequencies of wind turbine modes of interest that are used in the analysis.

Table 4.1: Frequencies of System Modes of Interest

Description	Value
Rotor frequency (1p frequency)	2.15 rad/s
Tower bending mode frequency	2.55 rad/s

Figure 3.3 shows open and closed-loop Bode plots from the wind disturbance to rotor speed deviation output. The closed-loop Bode plots show notably less gain at lower frequencies where the turbulent wind inputs have their highest magnitude. Both controllers have similar performance including a notch characteristic at the tower natural frequency. This notch characteristic is important to avoid exciting the tower bending mode.

Figure 4.1 shows the Bode plot from wind disturbance to M_{tilt}^{nr} . Here the baseline controller shows approximately 68 dB improvement at low frequencies compared with the disturbance augmented controller 86 dB improvement over the open-loop performance at low frequencies. Since the most dominant blade loads caused by $1p$ dynamics of the system get mapped to DC frequency after MBC transformation, both controllers are expected to achieve significant load reduction. The disturbance augmented con-

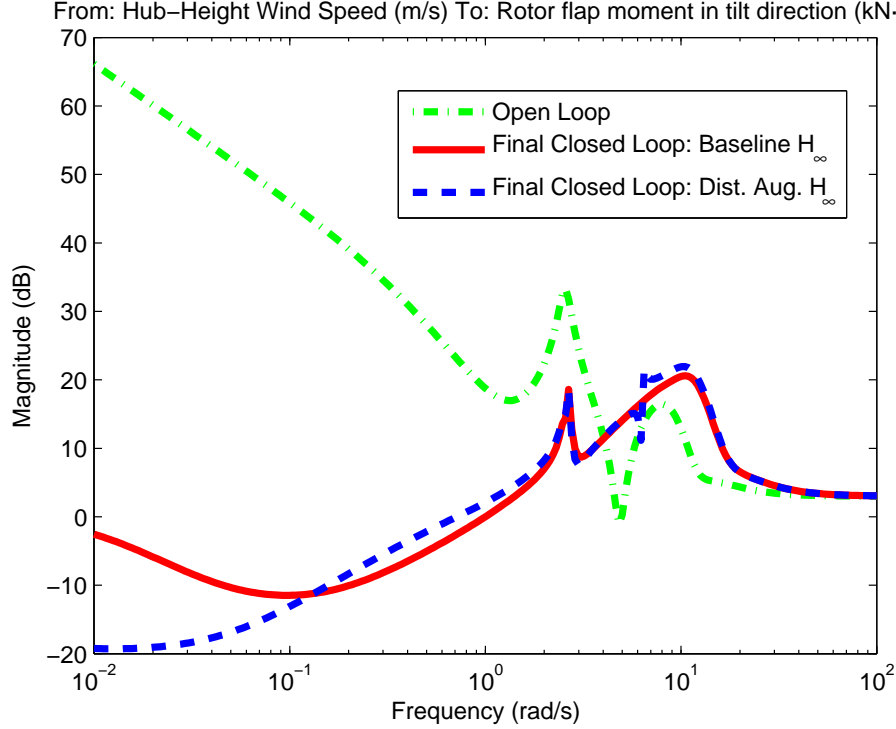


Figure 4.1: Bode Plots from Wind Disturbance to M_{tilt}^{nr}

troller shows slightly lower attenuation in the frequency range of 0.1-2.5 rad/s while showing a small improvement around $3p^{nr}$ frequency of 6.45 rad/s. This is due to low performance penalty at $3p^{nr}$ by W_{perf2} .

For M_{yaw}^{nr} , the baseline controller shows about 65 dB improvement and the disturbance augmented controller shows about 70 dB improvement at low frequencies (Figure 4.2). Characteristics of the controllers in this channel are identical to M_{tilt}^{nr} channel including the small improvement at the $3p^{nr}$ frequency by the disturbance augmented controller. These results indicate both controllers are expected to yield important fatigue reduction in yaw channel.

The disturbance augmented controller interconnection presented in Figure 3.4 included two additional disturbance inputs that drive the M_{tilt}^{nr} and M_{yaw}^{nr} outputs independently. The total disturbance rejection characteristics of individual pitch controllers depend on rejection of these output disturbances affecting M_{tilt}^{nr} and M_{yaw}^{nr} channels as well as rejection of wind disturbances. The Bode plot from disturbance acting on M_{tilt}^{nr} to M_{tilt}^{nr} output is given in Figure 4.3 and the yaw channel disturbance is given in Figure 4.4. The baseline controller shows about 45 dB improvement at

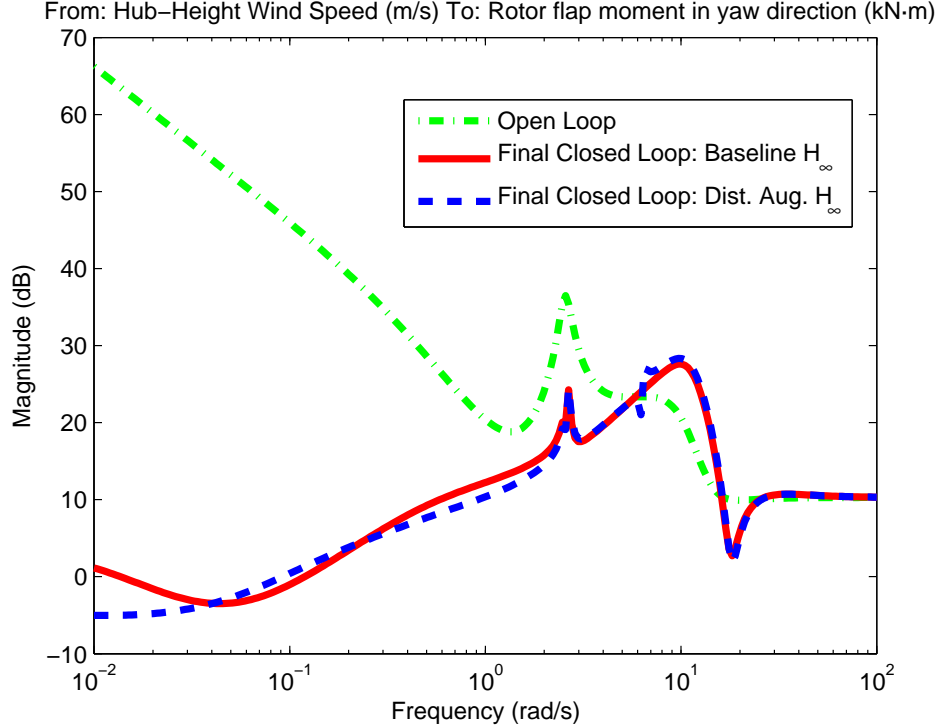


Figure 4.2: Bode Plots from Wind Disturbance to M_{yaw}^{nr}

low frequencies with negligible effect at $3p^{nr}$ mode in both channels. The disturbance augmented controller achieves an improvement of 65 dB improvement at low frequencies in nonrotating frame and also a limited improvement at $3p^{nr}$ dynamics just about 3 dB attenuation for both channels.

It is not straightforward to quantify the combined effect of linear disturbance rejection results on the nonlinear system response for arbitrary wind inputs. For steady wind conditions, the disturbance augmented controller is expected to cancel out $1p$ rotor dynamics better in the rotating frame, while $2p$ and $4p$ dynamics are expected to show slight improvement. If increased attenuation of blade oscillations is desired in steady wind conditions, the performance weights on M_{tilt}^{nr} and M_{yaw}^{nr} can be increased at $3p^{nr}$ frequency. This would improve attenuation at $2p$ and $4p$ frequencies.

4.2 Nonlinear Wind Turbine Simulations

The rotor speed and individual pitch controllers are simulated in the high order, 15 DOF nonlinear turbine model in FAST. The yaw dynamics are excluded from

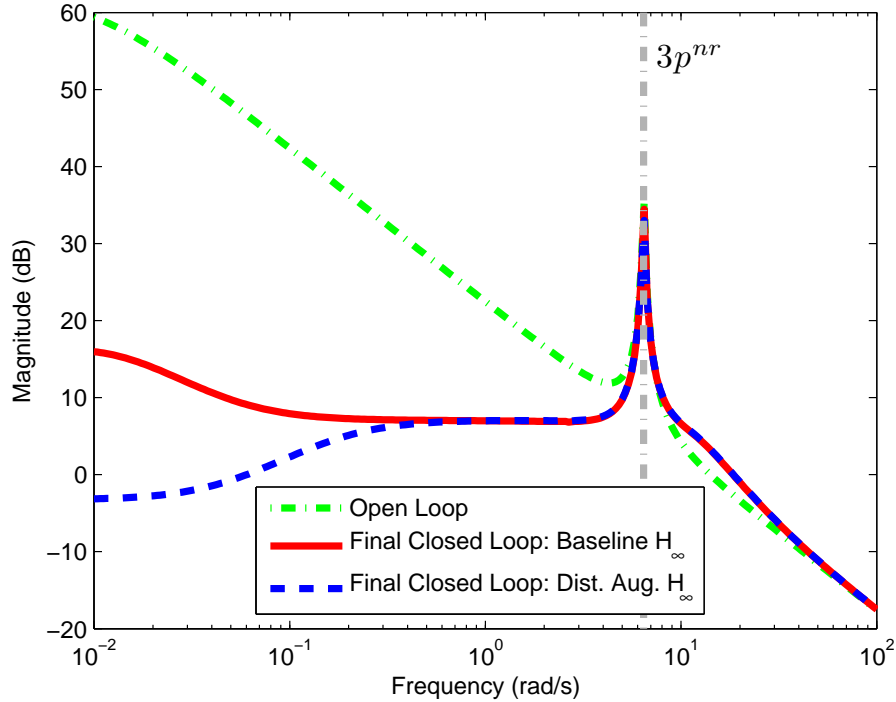


Figure 4.3: Open and Closed Loop Bode Plots for disturbance on M_{tilt}^{nr} to M_{tilt}^{nr}

the nonlinear model as discussed in Section 2.1. The simulations are conducted with steady wind conditions given in Table 2.1, and the addition of 1% and 5% turbulence to the steady winds. These turbulence levels are typically considered as low turbulence wind conditions by national and international wind turbine design standards. Dynamic inflow and dynamic stall effects are included in aerodynamic force calculations. The hub-height uniform wind component of the turbulent wind is given in Figure 4.5.

Blade fatigue characteristics are evaluated by comparing blade damage equivalent loads (DEL) using MCrunch [23], assuming a S-N curve (cyclic stress (S) versus number of cycles to failure (N)) slope of 10. Rotor speed tracking error is compared by calculating root-mean-square (RMS) deviations from the rated rotor speed using the time domain simulation results. The actuator usage is compared in time domain using the maximum value of pitch rate and RMS value of pitch rate of blades. The results are summarized in Table 4.2. Tower fatigue in fore-aft direction is also calculated to validate that the control law does not adversely affect the tower loads.

The power spectral density (PSD) obtained using the p-Welch algorithm of root

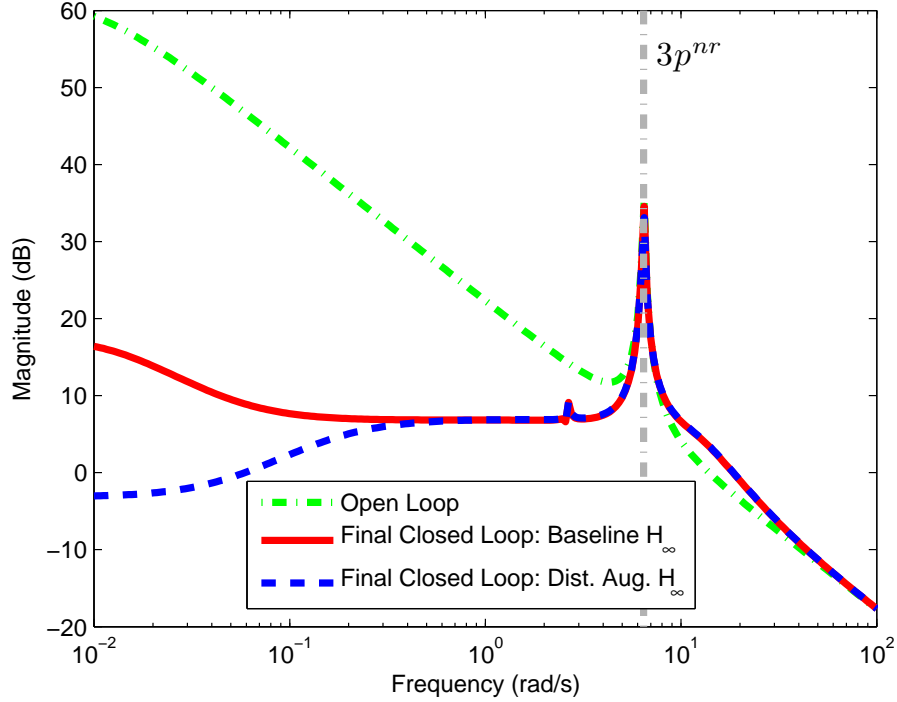


Figure 4.4: Open and Closed Loop Bode Plots for disturbance on M_{yaw}^{nr} to M_{yaw}^{nr}

bending moment of Blade 1 is presented in Figure 4.6 for steady wind conditions. Data sets for each simulation are divided into 12 segments with 50% overlap and a Hamming window is used as the window function. Figure 4.6 shows that under steady wind conditions most of the blade loading occurs at multiples of the rotor frequency, i.e. $1p, 2p, 3p, 4p$, and at the tower natural frequency. The disturbance augmented controller almost completely cancels out the $1p$ component of the load as well as improving results at $2p$ and $4p$ significantly. This agrees well with the choice of performance weight W_{perf2} which was heavily penalizing $0p^{nr}$ in nonrotating frame. Even though the W_{perf2} did not have a significant gain at $3p^{nr}$, the disturbance model has included $3p^{nr}$ components of the persistent disturbances. Hence controller shows some improvements at $3p^{nr}$ mode in nonrotating frame as well, which carries loads from $2p$ and $4p$ dynamics of the rotation as summarized in Table 3.1. If further reduction of loads at these frequencies are desired, the gain of the W_{perf2} can be modified to have a higher gain at $3p^{nr}$ frequency. The PSD of only the speed-regulated turbine (no IPC) is not included here since it carried a substantially large $1p$ and $2p$ components that rendered all other details of the plot indistinguishable. The peaks

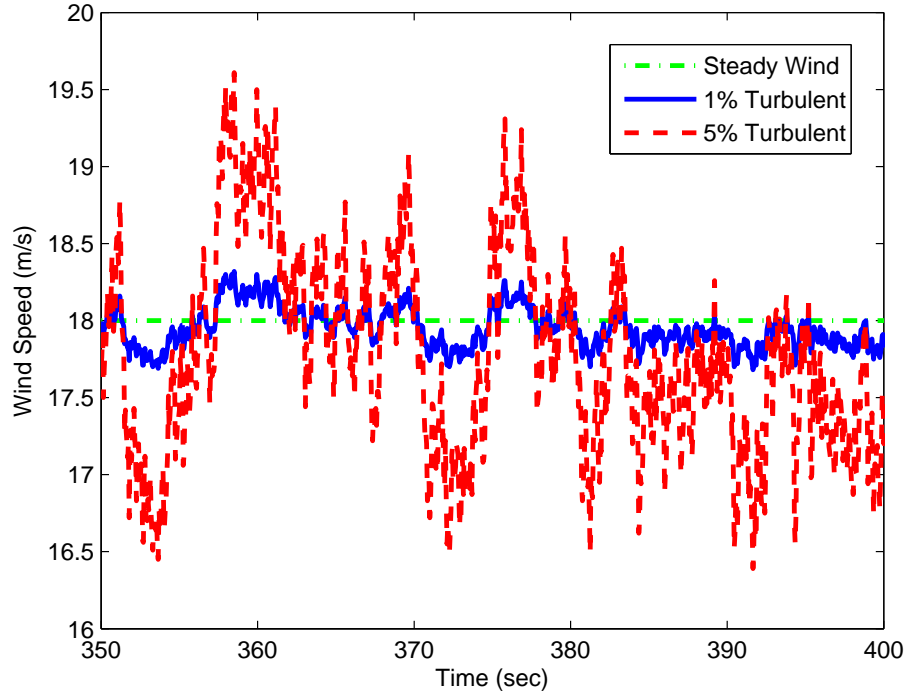


Figure 4.5: Hub-height wind disturbances used in simulations

of the PSD of the only speed regulated turbine occurred at 500000 for $1p$ and 2100 for $2p$ frequency compared to the values observed in Figure 4.6.

The PSD of Blade 1 root bending moment due to 1% turbulent wind conditions is presented in Figure 4.7. Figure 4.7 shows that with the inclusion of 1% turbulence, the peaks of the PSD no longer just occur at multiples of rotor frequency but also at frequencies where wind turbulence carries energy. Improvements by the disturbance augmented controller are still distinguishable at multiples at rotor frequencies. But the percentage-wise improvement is decreased due to increasing contribution to fatigue from M_{avg}^{nr} channel as well as loads at a wider frequency band in M_{yaw}^{nr} and M_{tilt}^{nr} .

The PSD of Blade 1 root bending moment under 5% turbulence is presented in Figure 4.8. At this point, improvements by disturbance augmentation are no longer distinguishable. The effects of wind turbulence are more pronounced and most of the blade loads are occurring at the low frequency range between 0 rad/s and 1 rad/s. Improvements by disturbance augmentation are indistinguishable and both controllers yield similar DEL.

Table 4.2: Controller Performance Comparison for Nonlinear Simulations

Description	Baseline H_∞	Dist. Aug. H_∞
Steady Wind		
Blade root flapwise DEL	38.52	33.07
Tower fore-aft bending DEL	130	132.7
RMS Rotor Speed Error (rad/s)	0.033	0.033
RMS Pitch Rate (rad/s)	0.036	0.036
Max Pitch Rate (rad/s)	0.063	0.064
1% Turbulent Wind		
Blade root flapwise DEL	100.2	98.80
Tower fore-aft bending DEL	538.8	539.8
RMS Rotor Speed Error (rad/s)	0.059	0.059
RMS Pitch Rate (rad/s)	0.037	0.037
Max Pitch Rate (rad/s)	0.078	0.080
5% Turbulent Wind		
Blade root flapwise DEL	452.7	453.2
Tower fore-aft bending DEL	2687	2692
RMS Rotor Speed Error (rad/s)	0.265	0.265
RMS Pitch Rate (rad/s)	0.042	0.042
Max Pitch Rate (rad/s)	0.146	0.155

The PSD of the M_{avg}^{nr} and M_{tilt}^{nr} channels under steady, 1% turbulent and 5% turbulent wind are given in Figure 4.9 and 4.10 respectively. Figure 4.10 shows that the asymmetrical loads on rotor are spread over a wider frequency range in M_{tilt}^{nr} channel. Figure 4.9 shows that the ratio of the loads in M_{avg}^{nr} channel to the loads in M_{tilt}^{nr} channel increases rapidly. Hence any improvement obtained in M_{tilt}^{nr} and M_{yaw}^{nr} channels becomes less significant as the bending moment of Blade 1 is $M_1 = M_{avg}^{nr} + \sin(\psi_r(t))M_{avg}^{nr} + \cos(\psi_r(t))M_{yaw}^{nr}$ from Eqs. 2.10 and 2.12. Both of these issues are effects not addressed by the disturbance model augmentation since disturbance augmented design achieves load reduction improvements only at the multiples of the rotor frequency in the M_{tilt}^{nr} and M_{yaw}^{nr} channels. Thus the diminishing importance of the load reduction obtained through disturbance augmented design is regardless of the design of the disturbance augmented controller. Moreover, this phenomena even occurs at low turbulence levels such as 1% which is typically lower than the turbulence levels observed at wind farms.

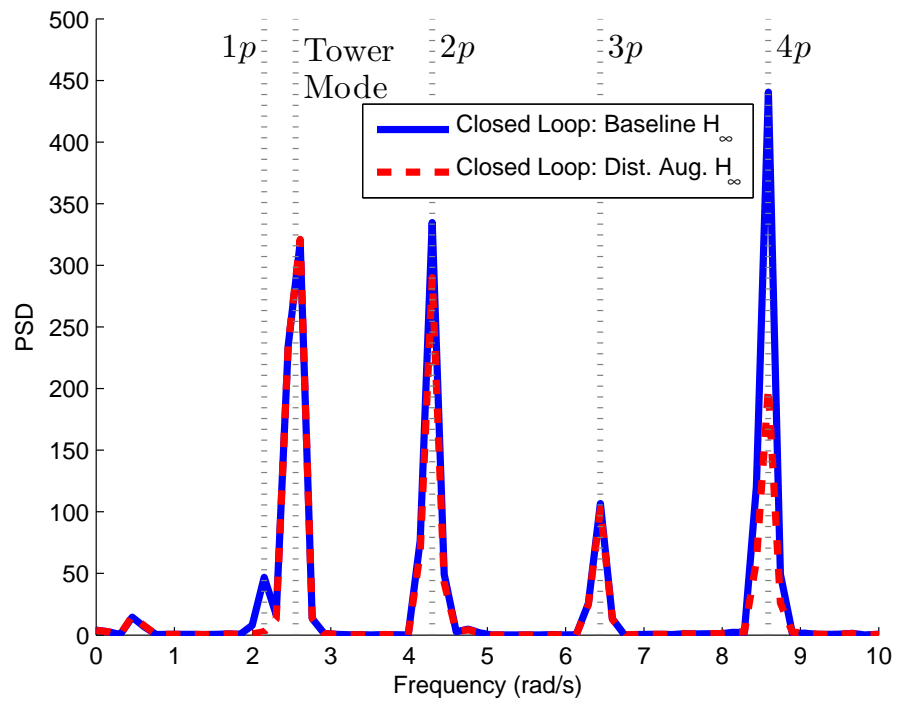


Figure 4.6: PSD of Blade 1 Root Bending Moment under steady wind conditions

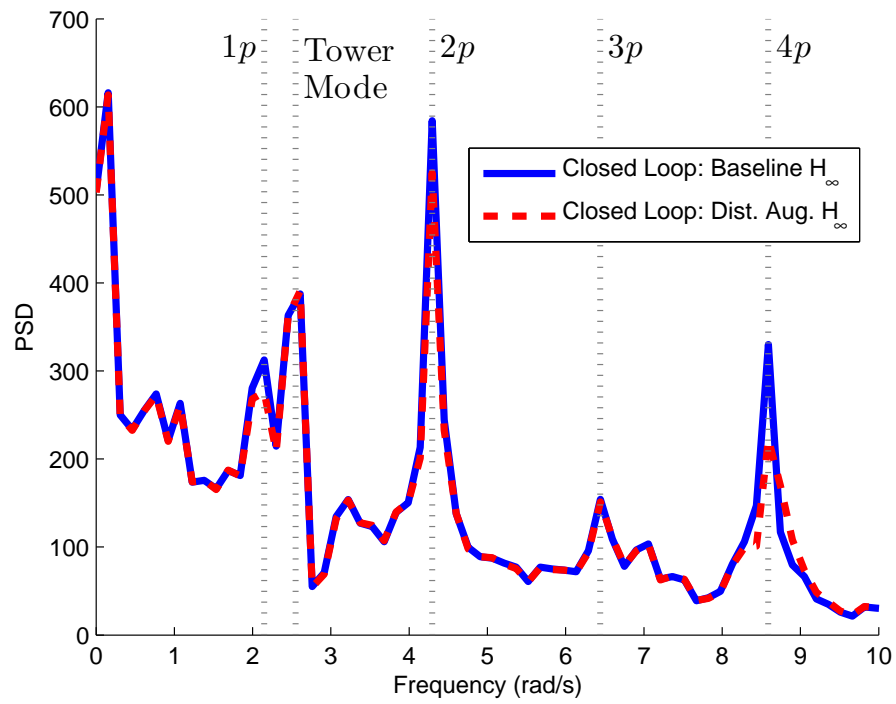


Figure 4.7: PSD of Blade 1 Root Bending Moment under 1% turbulent wind

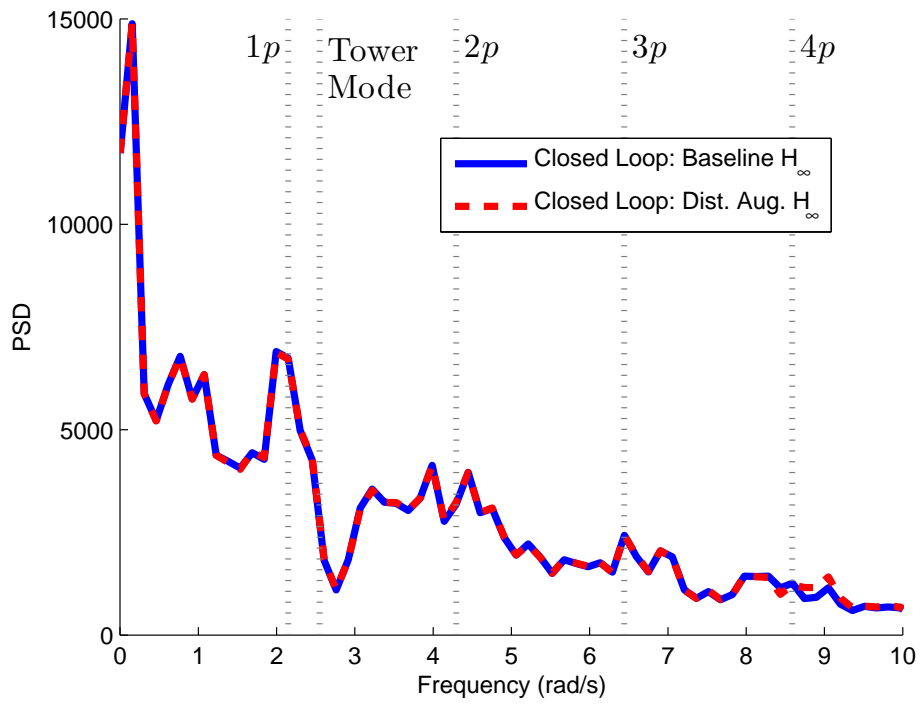


Figure 4.8: PSD of Blade 1 Root Bending Moment under 5% turbulent wind

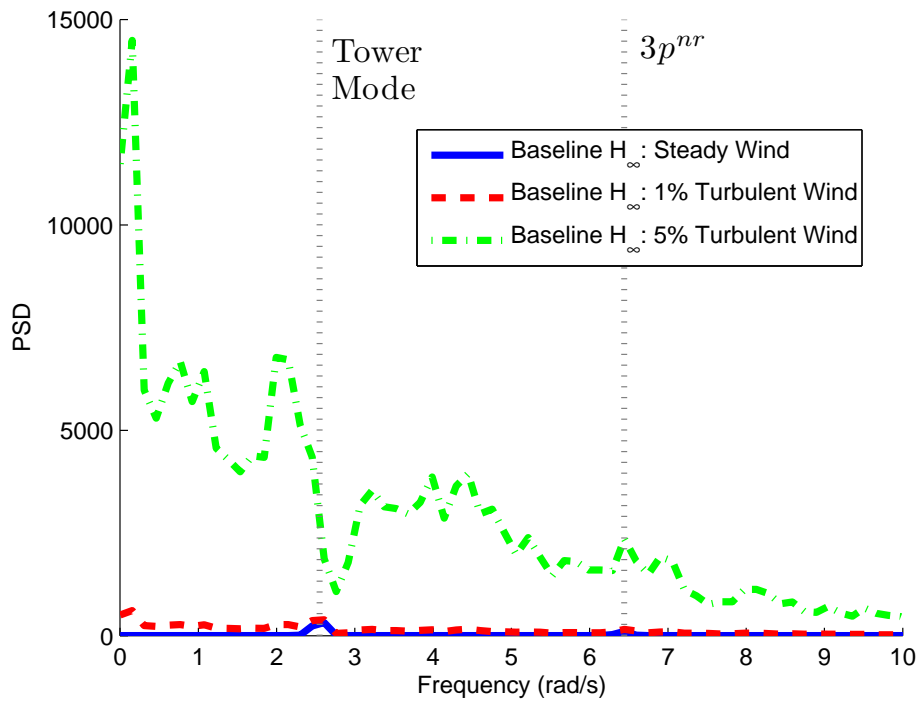


Figure 4.9: The PSD of M_{avg} Channel

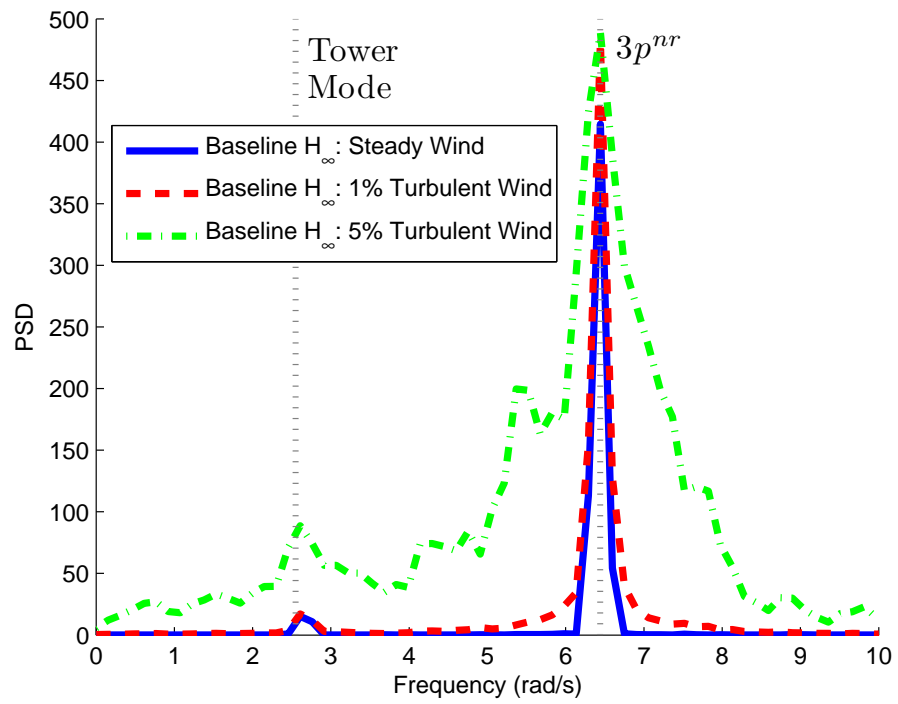


Figure 4.10: The PSD of M_{tilt} Channel

Chapter 5

Conclusions

This paper investigates the effects of disturbance model augmentation for individual pitch control design. In the literature, disturbance augmentation is used for accommodating persistent disturbances causing loads at the multiples of the rotor frequency. A baseline H_∞ controller was designed for individual pitch control and compared to a second controller that incorporates a disturbance model into design procedure. The effects of the added disturbance model were investigated through linear analysis as well as nonlinear simulations presented in time and frequency domains. Results show that augmenting the disturbance model yields performance improvements at steady and low turbulent wind conditions. Though both controllers yield similar performance characteristics as the turbulence increases. This is due to the high collective loading of the blades caused by turbulence which is not addressed by the IPC algorithms. In addition, as energy from the turbulent wind conditions spreads through a broader frequency spectrum, improvements obtained at multiples of the rotor frequency are less important. Hence disturbance model augmentation may not yield expected performance improvements under turbulent wind conditions.

Acknowledgments

This work was supported by the University of Minnesota Institute on the Environment, IREE Grant No. RS-0039-09, the US Department of Energy Contract No. DE-EE0002980 and the US National Science Foundation under Grant No. NSF-CNS-0931931. Any opinions, findings, and conclusions or recommendations expressed in this material are those of the author(s) and do not necessarily reflect the views of the University of Minnesota, Department of Energy or National Science Foundation.

Bibliography

- [1] Bossanyi, E. A., “The design of closed loop controllers for wind turbines,” *Wind Energy*, Vol. 3, No. 3, 2000, pp. 149–163.
- [2] Bossanyi, E. A., “Individual Blade Pitch Control for Load Reduction,” *Wind Energy*, Vol. 6, No. 2, 2003, pp. 119–128.
- [3] Geyler, M. and Caselitz, P., “Robust Multivariable Pitch Control Design for Load Reduction on Large Wind Turbines,” *Journal of Solar Energy Engineering*, Vol. 130, No. 3, 2008, pp. 031014.
- [4] Johnson, C. D., “Theory of Disturbance-Accommodating Controllers,” *Control and Dynamic Systems*, Vol. 12, 1976, pp. 387–489.
- [5] Stol, K. A. and Balas, M. J., “Periodic Disturbance Accommodating Control for Blade Load Mitigation in Wind Turbines,” *Journal of Solar Energy Engineering*, Vol. 125, No. 4, 2003, pp. 379–385.
- [6] Wright, A. D. and Balas, M. J., “Design of Controls to Attenuate Loads in the Controls Advanced Research Turbine,” *Journal of Solar Energy Engineering*, Vol. 126, No. 4, 2004, pp. 1083–1091.
- [7] Laks, J. H., Pao, L. Y., and Wright, A. D., “Control of Wind Turbines: Past, Present, and Future,” *Proceedings of American Control Conference*, St. Louis, Missouri, 2009, pp. 2096–2103.
- [8] Stol, K. A., *Dynamics Modeling and Periodic Control of Horizontal-Axis Wind Turbines*, Ph.D. thesis, University of Colorado at Boulder, Boulder, Colorado, 2001.
- [9] Johnson, W., *Helicopter Theory*, Princeton University Press, 1st ed., 1980.

- [10] Coleman, R. and Feingold, A., “Theory of Self-excited Mechanical Oscillations of Helicopter Rotors with Hinged Blades,” Tech. rep., NASA, 1958.
- [11] Stol, K. A., Moll, H.-G., Bir, G., and Namik, H., “A comparison of multi-blade coordinate transformation and direct periodic techniques for wind turbine control design,” *Proceedings of the 47th AIAA/ASME*, Orlando, Florida, 2009, pp. AIAA–2009–479.
- [12] Jonkman, J. M. and Buhl, J. M. L., *FAST User’s Guide*, National Renewable Energy Laboratory, Golden, Colorado, 2005.
- [13] Hansen, A. C., *Users Guide to the Wind Turbine Dynamics Computer Programs YawDyn and AeroDyn for ADAMS version 11.0*, Mech. Eng. Dept. University of Utah, Golden, Colorado, 1998.
- [14] Stol, K. and Balas, M., “Full-State Feedback Control of a Variable-Speed Wind Turbine: A Comparison of Periodic and Constant Gains,” *Journal of Solar Energy Engineering*, Vol. 123, No. 4, 2001, pp. 319–326.
- [15] Selvam, K., Kanev, S., van Wingerden, J. W., van Engelen, T., and Verhaegen, M., “Feedback-feedforward individual pitch control for wind turbine load reduction,” *International Journal of Robust and Nonlinear Control*, Vol. 19, No. 1, 2008, pp. 72–91.
- [16] Bir, G., “Multi-Blade Coordinate Transformation and Its Applications to Wind Turbine Analysis,” *AIAA Wind Energy Symposium*, Reno, Nevada, 2008, pp. AIAA–2008–1300.
- [17] Doyle, J., Glover, K., Khargonekar, P., and Francis, B., “State-space solutions to standard H_2 and H_∞ control problems,” *IEEE Transactions on Automatic Control*, Vol. 34, No. 8, aug 1989, pp. 831–847.
- [18] Zhou, K., Doyle, J. C., and Glover, K., *Robust and Optimal Control*, Prentice Hall, 1st ed., 1996.
- [19] IEC 61400-1, “Wind turbines-Part 1: Design requirements,” Tech. rep., International Electrotechnical Commission, 8 2005.
- [20] Burton, T., Sharpe, D., Jenkins, N., and Bossanyi, E., *Wind Energy Handbook*, John Wiley & Sons, 1st ed., 2001.

- [21] Jonkman, B., *TurbSim User's Guide*, National Renewable Energy Laboratory, Golden, Colorado, 2009.
- [22] Arcara, P., Bittanti, S., and Lovera, M., "Periodic control of helicopter rotors for attenuation of vibrations in forward flight," *IEEE Transactions on Control Systems Technology*, Vol. 8, No. 6, nov 2000, pp. 883–894.
- [23] Buhl, J. M. L., *MCrunch User's Guide*, National Renewable Energy Laboratory, Golden, Colorado, 2008.